

Towards a biohybrid brain-machine interface: Formulation of an engineering process framework implemented in newly modelled PDMS designs

INI-506: Short Project II

11.2020 - 02.2021

Simon Steffens

Abstract

Capable brain-machine interfaces are the foundation for progress in neuroscience research, medical treatment of the brain and thought provoking black mirror episodes. In Moore's law fashion, the density at which we can record single neuron activity *in vivo* has doubled every seven years over the last 60 years (albeit partially ignoring spatiotemporal resolution). On the contrary, current electrode technology is incapable of stimulating multiple neurons at single cell resolution *in vivo*. We will overcome this problem by employing a tissue-engineering approach: Instead of relying on metal electrodes limited to expansive stimulation, our biohybrid multielectrode array (bioMEA) uses *in vitro* grown ectopic neurons whose axons innervate the region to stimulate. In simple terms, the implant consists of a PDMS (silicone) guidance microstructure that directs the ectopic axons into the implanted tube. Below the guidance channels is a stretchable electrode array that enables us to stimulate our neurons electrically and send action potentials to the implanted brain region.

The initial motivation of the sub-project presented here emerged from criticism pointing out the overwhelming complexity in engineering this biohybrid interface. Given the difficulties involved when building with biological parts, we asked how should one approach this complex engineering task such that chances of success are maximal. The answer provided by this work is a framework that decomposes the engineering process into sub components that are iteratively optimized using a high-throughput debugging platform. Due to the multitude of parameters to consider in our device, the efficiency at which we are able update the prototype is likely going to determine the success of the project. A significant amount of time was therefore invested in modelling new axon guidance structures. Crucially, the new layout of PDMS structures permits specialized experiments and testing with higher throughput. Moreover, the modelled PDMS mask includes 20 new implant designs that address the issue of non-directional growth through the guidance structure resulting in decreased bandwidth and cross-talk between electric channels. Incorporating channel connectivity, attractor cue gradients and specific guidance motifs into the design model, the new structures should exhibit highly improved directional axonal growth towards the implanted tube. All in all, this work shows the feasibility, and lays a foundation for building a stimulating biohybrid multielectrode array, ensued by taking first practical steps by designing a new PDMS wafer for fabrication.

Contents

1	Introduction	1
1.1	High level overview	1
1.2	Low level overview	2
2	Engineering process framework	3
2.1	Parameters	3
2.2	Metrics	4
3	General aspects of PDMS mask design	4
3.1	Design goals and implementations	4
4	PDMS designs optimizing directional growth	6
4.1	Parameterizing PDMS designs	6
4.2	Conceptualizing axonal outgrowth as a Markov chain	6
4.2.1	Grouping dependent parameters based on the Markov model	7
4.3	Deriving parameter value combinations from the Markov model	8
4.3.1	i: Node frequency & connectivity	9
4.3.2	ii: Transition probabilities - cue gradient	9
4.3.3	iii: Transition probabilities - axon-axon interaction	10
4.3.4	iv: Transition probabilities - PDMS design motifs	10
4.4	Further experiments	12
5	Discussion	13
6	Supplementary Information	13

1 Introduction

1.1 High level overview

This work is a contribution to the more comprehensive endeavor of building a brain machine interface using ectopic axons as electrodes. As this work addresses fine-grain engineering problems, one first needs to get a general overview of the device, its components, and the assembly process to appreciate the results presented here. Before going into the underlying details of the device though, we may want to ask why this is a relevant project to work on in the first place. At the lowest level, the device is motivated by the fundamental wall researchers and biomedical engineers face, regarding high-density stimulation of the brain with spatial resolution beyond large neural populations.

While recording technologies have made considerable progress over the last years, stimulation methods have not kept up. In the medical domain, deep brain stimulation of basal ganglia has received a lot of attention over the last decade, especially due to the remarkable improvements for patients suffering from Parkinson disease (PD). Still, these systems suffer from a range of shortcomings: first and foremost, the spatial resolution of stimulation is limited to neural populations or entire nuclei, second, immunoreaction to the implanted electrodes causes complications in the long term, and lastly, these systems are limited in their adjustability post surgery, as voltage and pulse width are the only tunable parameters. In research applications, brain stimulation is dominated by optogenetic methods. Similar to electrical deep brain stimulation, this technology comes with spatial limitations imposed by the nature of light. On top of that, optogenetic stimulation requires genetic engineering in the target region, currently still a notable hurdle for any medical application. Our biohybrid multielectrode array (bioMEA) aims to achieve stimulation at single-neuron resolution while simultaneously resolving the latent issue of biocompatibility encountered with implanted metal electrodes. Such single-cell resolution interfaces are strictly required for delivering high dimensional information, for example from the sensory domain. This is the initial area of application we intend to target with this device, specifically, restoring the visual input to the dorsal lateral geniculate nucleus (dLGN) as depicted in Figure 1 below.

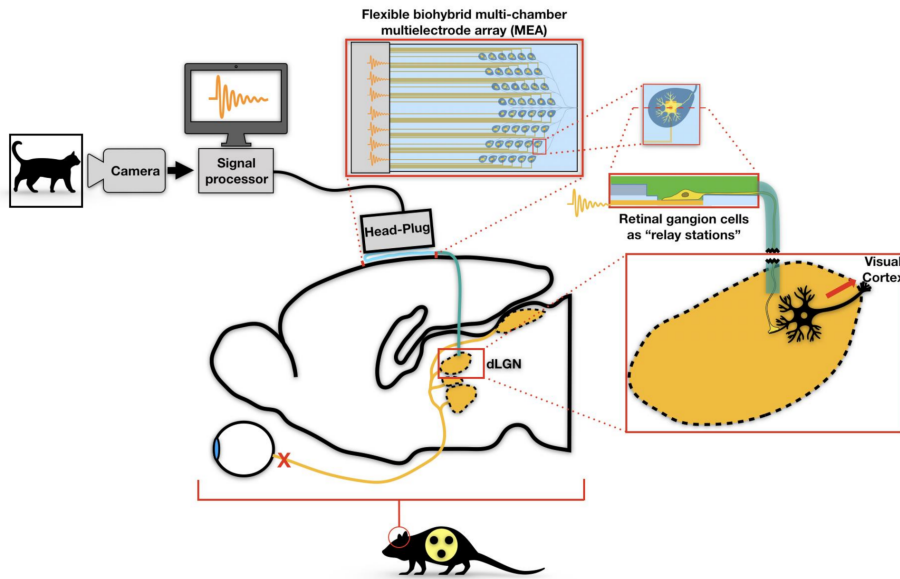


Figure 1: We prepare the implant *in vitro*, with axons already inside the structure. The device is then implanted under the skull such that ectopic neurons face down to receive nutrients from the brain surface; the guiding axon channel terminates in dLGN. We hope that the combined effect of absent input from the optic nerve (dissected) and applying stimulation through the interface induces the formation of functional synapses. The animals age and the time interval from optic nerve dissection to implantation is likely to be critical for this to occur. In a final application, the interface is connected to a neuromorphic chip that functions as an artificial retina processing raw camera signals.

How does the current prototype device work? We start by preparing the PDMS structures which house and guide the ectopic neurons. These 250 μm x ~2 mm x ~5 mm (z, x, y) structures implement the source wells for ectopic neurons from which 6 μm high tracts extend out of. In the final device, these 6 μm axonal tracts run over stretchable AuTiO₂ nanowire electrical contact pads that enable stimulation of neural electrical activity by depolarizing the axon above it. However since manufacturing these PDMS-based stretchable electrode arrays is challenging, we currently place our structures on glass multielectrode arrays (Multichannel Systems MCS GmbH) to measure and induce electrical activity. The 6 μm axon channels connecting to the source wells converge into the 3 mm long output channel which will eventually be implanted. For optimal biocompatibility and fast growth, a nanofiber tube will be used for this in the future, but in the current design iteration we simply use a wider and higher PDMS channel. To attract axons towards this output channel, we place a piece of thalamic tissue on the 3 mm output channel (has small openings) so that emitted cues can diffuse into the PDMS structure.

This PDMS 'lobe' is placed in a glass well (or the glassMEA when electrical interfacing is required) that has been coated with laminin and poly-D-lysine to facilitate growth. In past designs, we seeded dissociated primary retinal ganglion cells (RGCs) obtained from E18 rat retinas, but for neural viability and simplicity reasons, we recently moved to larger source wells that house retinal tissue pieces of size 300 μm x 300 μm . Axons elongate at a speed of about 400 $\mu\text{m}/\text{day}$ and usually reach the end of the 3 mm long output channel within two weeks.

1.2 Low level overview

As might be apparent from the outline above, building this bioMEA for neural interfacing is a challenging engineering problem with a multitude of potential obstacles in the way; it is not clear that our orthogonal approach to building a CNS stimulation device is tractable. Given the general unpredictability when doing engineering with biological parts, one may critically ask why this has a chance to succeed. In a way, the first results section of this report can be interpreted as answering a related, more productive question: how should this problem be approached if we aim for maximizing the probability of success? Coming from the very realization that we picked a difficult engineering problem, one motivation of this work was to come up with a systematic engineering process that at the end yields a working prototype. The prototype device should exhibit minimal cross talk between channels, RGC survival on a timescale of months, and most importantly, the ability to form functional synapses on thalamic tissue *in vitro*. In **section 2**, we formulate a simple engineering framework from which a potential experimental roadmap derives. This formulation of the engineering process enables one to split the problem in smaller, approachable tasks, allowing for iterative, parallelized optimization of isolated components.

To effectively execute on the experimental plan that derives from this framework, new PDMS designs are indispensable. A central argument made by this report is that we need to move towards high-throughput, efficient experimental cycles to optimize the device on a reasonable timescale. Achieving this is strongly contingent on smart PDMS structure layouts that permit fast testing. Motivated by this assigned significance, one entire month of this three month project was dedicated to planning and modelling a new PDMS wafer, which is explained in **section 3** (remaining two months were spent learning practical protocols). We model the desired 2D channel structure in CAD using Fusion360, AutoCAD and KLayout. This design is rendered as a .gds2 file to create the fabrication mask. We send this mask design to Wunderlichips GmbH, a private company that fabricates the silicon wafer using SU-8 mold photolithography. The wafer has a diameter of ~10 cm allowing us to arrange the single implant structures in a grid like pattern (see Suppl. Figure 12 for the complete new wafer design).

Besides general optimization of the experimental throughput through the PDMS wafer design, this work describes 20 new PDMS structures and the conceptual model behind the design process (**section 4**). These specific implant designs aim to solve an immediate problem we currently experience with our PDMS structures: directional growth. Ideally, we want all axons originating from the source wells to grow into the tube that will eventually be implanted. However right now, a great number of them grow towards neighboring seeding wells. Incorporating optimal tract connectivity, cue gradients and PDMS motif designs in the design process, the new microstructure designs assure unidirectional axonal growth towards the implanted tube (in the final device made from nanofibers, right now PDMS).

Note that due to length limitations, integration with existing literature and discussion are kept to a minimum.

2 Engineering process framework

The following is an attempt to structure the optimization process towards a working bioMEA prototype. At the basis of the proposed engineering process structure lays a categorization into **parameters** and **metrics** (Figure 2). The instantiation of a parameter may correlate with one or a set of metrics, indicating the relevance of that parameter. Valid parameters need to have instantiations that can be directly implemented in the assembly process or the design itself, metrics need to be observable through some screening method. We could imagine the addition of a growth factor into the medium as a parameter with different concentrations as instantiations. The corresponding experiment would then involve a systematic screen for a set of predefined metrics, for example including long term neural viability and axonal outgrowth speed to identify the ideal concentration. The proposed framework on engineering an intricate system may seem trivial, however, this simple foundation is useful because it can enable one to perform a more structured search process (define the experimental plan) once the screening methodology has been established. Using this simple framework, we can conceptualize the engineering process as an optimization problem where we first come up with promising parameters, then search for the set of parameter instantiation that maximizes a set of metrics.

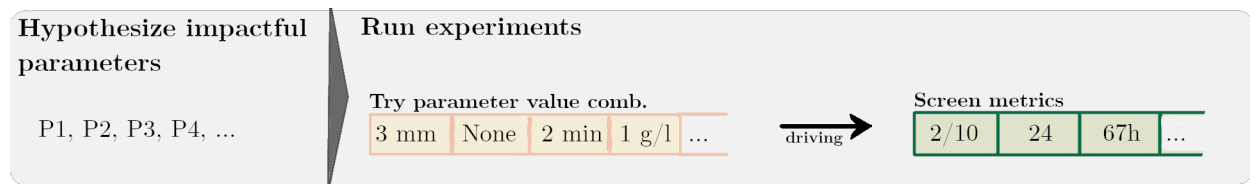


Figure 2: General design framework.

2.1 Parameters

Defining the parameter space is a challenging task in any engineering problem. Selecting parameters is a challenge, as technically anything in a design may be altered; from materials to fabrication methods, to fundamentally different PDMS structure designs. To make an engineering problem tractable, we rely on preexisting data to determine our initial set of parameter values. For example in our design, we define PDMS as a fixed parameter. The material is an instantiated, fixed parameter on which we built on. From there, we consider more high-level parameters, for example the tract width in the PDMS structure. As this example illustrates, parameters are often defined on top of more low-level parameter instantiations. This is relevant because while a design decision may seem optimal at an early stage of the engineering process, it may prevent good solutions for later parameter optimization that indirectly depend on this early decision. In summary, to build a complex system, one needs to carefully review low-level parameters as they define the realizable higher level parameters. In a way, the whole project can be seen as revising the low-level parameter of 'electrode-type', moving from tungsten to axons. Leaps of progress often emerge from rethinking these low-level parameters.

Within the process of finding ideal parameter instantiations, the interdependence between parameters also needs to be carefully assessed. Parameters often interact with each other in the way they drive the metrics. Thus, it is not enough to come up with a list of parameters and find their optimal value in a parameter specific experiment. Instead, experiments need to address these interdependencies by testing combinations of parameter values. To not end up with an intractable combinatorics problem, one needs to make assumptions about the independence and interdependence of parameters.

A major part of this work has focused on the analysis of separating independent parameters that drive directional axonal growth. These parameters (eg. axon tract width, channel joint motifs design, etc.) are discussed in great detail in section 4. Besides these PDMS design specific parameters, potential parameters to optimize include **medium composition**, **surface coating**, and **medium exchange cycle**. When we widen the definition of a parameter slightly, we may also consider **myelination** effects through the addition of oligodendrocytes, **reusing structures** that already had axons grown on them, **contralateral growth** of two structures (see section 4.4 for details), **timepoint of retinal collection**, and the **preparation of**

retinal tissue (single-cell vs explant). These are not parameters in the classical sense, however, they still follow the model in that we design experiments that test the value of a binary factor by screening the metrics. Another interesting parameter would be the **elapsed time from retinal dissection to RGCs seeding** onto the implant, testing timescales of hours to weeks.

2.2 Metrics

Defining the metrics for our initial prototype is relatively straight forward as they directly derive from the desired functionality of the implant. First, the prototype should exhibit **directional growth** through the PDMS channel structure. When this is not given, we end up with cross-talk between axonal channels decreasing bandwidth and worse, possibly causing undesired activity dynamics within the device due to functional connectivity between neighboring RGC source containers. Secondly, the quality of a particular set of parameter instantiations is given by the **long-term survivability** of the seeded retinal ganglion cells. Since the implant needs to be long-term stable, this is an important metric. The third metric is signal **transmission efficacy** through the device to stimulate the target tissue. Lastly is **axonal outgrowth** frequency and speed, which is mainly contributing to the ability to quickly test devices but may also be an indicator of neural health and efficacy. While defining the metrics is simple, developing reliable and fast screening methods that quantify these is not. This problem will be addressed in future work.

In sum, we derive a concrete experimental plan from the parameters and metrics summarized in Figure 3 below. Once the screening methodology has been established, we can rapidly iterate through parameter value combinations that will lead to a working prototype implant.

Parameters	Metrics
[PDMS guiding structure design] medium composition (multi dim.) surface coating (multi dim.) medium exchange cycle myelination	reusing structures contralateral growth timepoint of retinal collection preparation of retinal tissue elapsed t retina collection - seeding

Figure 3: Summarization of parameters and metrics outlined above. Collection of [PDMS design specific parameters] are listed in Figure 5. (multi-dim) indicates that these parameters are composed of multiple sub-parameters, eg. a list of components for the medium.

3 General aspects of PDMS mask design

So far, we have formulated a low-level framework to structure the engineering process and we have defined a set of explicit metrics and (non-PDMS related) parameters. A particular focus of this short project was put on the design of a new PDMS mask as this design forms the basis for realizing experiments within the framework above. It is the first step to enable one to systematically test the impact of hypothesized parameters, parameter instantiations, and establish standardized screenings. The following section outlines the details of designing the PDMS mask according to a set of design goals. Here, we still exclude parameters regarding specifics in the PDMS designs, for example the axon tract width. Instead, we focus on the layout of structures and general desirable features in the PDMS structures.

3.1 Design goals and implementations

A central goal of the new PDMS mask was to **enable higher throughput experiments (i)**. Given the complexity of the device we are building, an efficient parameter optimization and debugging cycle is essential. An intuitive way to increase the throughput of experiments is to decrease assembly time of the device. Currently, we place one PDMS structure in one glass well. Every glass well needs to be assembled,

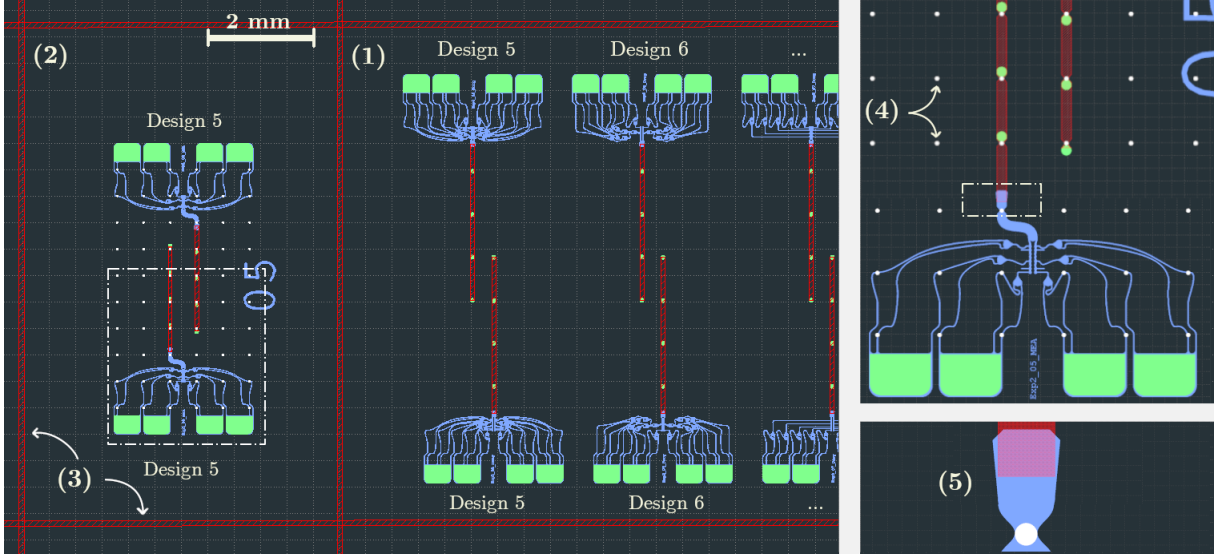


Figure 4: Subsection of the PDMS wafer. Colors indicate heights of PDMS channels: blue = 6 μm , red = 75 μm , green = opening. (1) 8-stack structure with implant designs 5-8 (details are explained in the next section). Two of the 8 designs are cut off in this image. (2) 2-stack structure of design 5 fitting the glassMEA by removing 8 of the 20 channels, but keeping the rest conserved. (4) Indicates electrical contact pads of the glassMEA. This is just included for illustrative purposes, in the final mask these are omitted. (5) Due to fabrication constraints, different height-layers of the wafer might be slightly shifted with respect to each other. Using this specific connection motif between two different heights, a slight shift of the 75 μm channel in any direction will not change the growth-relevant transitions angles between layers. This contributes to increased experimental throughput, as reliability in assembling the device increases.

coated, mounted, seeded, the medium needs to be exchanged and we can only image this one structure at a time. The solution provided here is quite simple. Instead of using single structures, the new PDMS mask contains 8-stack composition structures that still fit into the glass well (Figure 4 (1)). By stacking the structures, we reduce assembly time by 8 folds, and imaging multiple structures becomes far more convenient. Assembly time is further decreased and made more reproducible by outlining different stacks with cut lines on the mask to have a laser cutter slice them (Figure 4 (3)).

Besides these layout related features, we may also consider general design goals for the specific PDMS implant structure designs. In accordance with the framework defined above, the chief design goal for any structure is to **optimize the metrics (ii)**. This aspect is discussed in the next section. Beyond this primary goal, there are other desirable properties we should consider implementing in the structure designs. One obvious example is to **maximize bandwidth (iii)** in our device, or more concretely, maximize the number of independent axonal channels exiting the RGC source containers. This is not too relevant for building a working prototype but we should still be explicit about this design goal as it defines the resolution of our implant in the future. Another important feature in our designs should be versatility with respect to the **electrical interface (iv)** being used. As outlined in the introduction, we may use glass multielectrode arrays (glassMEA) from Multichannel Systems to record and induce neural electrical activity *in vitro*. The contact pads of these devices are fixed, hence we need to fit our designs to the grid of contact pads on the glassMEA. At the same time, we would prefer designs that are also compatible with the intended final solution for electrical interfacing, a stretchable array of AuTiO₂ nanowires embedded in PDMS. An example of how this was achieved is illustrated in Figure 4: Each structure design has two versions, one that fits the glassMEA (Figure 4 (2)), and one more dense version that would work with the final stretchable electrode array (Figure 4 (1)). Importantly, these designs are equivalent in any aspect except their channel density. Thus, we may screen the lower density structure version electrically using the glassMEA (2-stack), or we could screen the higher density version using microscopy methods (8-stack). In CAD, the designs were planned such that one could model the dense versions first, then simply move to the glassMEA version by

deleting superfluous channels. Given that we ended up with 20 different designs to model, this trick in the workflow was absolutely essential. Lastly, we want to minimize **implant size (v)** and stick to a **strip-like form factor (vi)** to facilitate surgical implantation in the future.

4 PDMS designs optimizing directional growth

Up to this point, we have only discussed the PDMS designs from a general perspective without a particular focus on the framework of parameters and metrics. This section covers exactly that. How should we design PDMS structures to optimize our predefined metrics? Which parameters may act as positive drivers? First, we should consider how the PDMS structure design could affect the metrics. While neural viability, functional efficacy, and axonal outgrowth speed may be marginally affected by the details in the PDMS structures, the metric chiefly affected by the structure design is directional axonal growth. This has been the leading question behind the PDMS design process. How can we design structures in which axons grow from the source well into the output channel instead of innervating neighboring wells causing channel cross talk in the device.

4.1 Parameterizing PDMS designs

To find a PDMS design with minimal cross talk between channels, one needs to first define a set of design parameters that are likely to determine directional axonal outgrowth. In accordance with the conceptual model explained in the next section, the PDMS designs are parameterized into the following ten factors (also see Figure 5): number (**P1**) and placement (**P3**) of joints before the final joining lane, number of rescue loops (**P2**), placement of the final joining lane (**P4**), channel width (**P5**), distance to the attractor slice (**P6**), and finally the design of rescue loops (**P7**), normal joints (**P8**), final lane joints (**P9**) and integration of spiky tracts (**P10**).

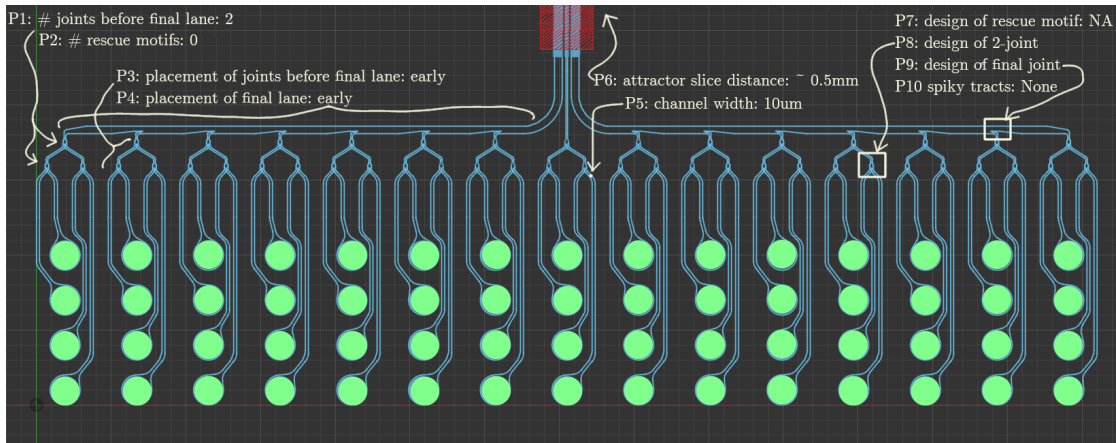


Figure 5: Current PDMS design with parameters annotated. The design above uses single cell wells, whereas the new structures rely on explant containers.

Obviously, CAD modelling and screening all combinations of these ten parameters even with an average of only three values per parameter is unrealistic. This combinatorial problem is addressed by grouping parameters into causally interdependent sub-components according to the model below.

4.2 Conceptualizing axonal outgrowth as a Markov chain

Having a conceptual model of the problem to solve may help to discern (in)dependencies within the large PDMS design parameter space. When thinking of axons growing from some starting point through a channel system with multiple junctions, Markov chains intuitively come to mind. The idea behind these stochastic

models is fairly simple: we can model a sequence of transitions from one state to another where the probability of transitioning to the next state solely depends on the current state. We can therefore think of axonal outgrowth as a discrete random process where, for example, at any T-junction, the axon may transition into two different states: towards the output channel, or a neighboring well (Figure 6A). We can reformulate the problem as a random process where we want to maximize the probability that the source nodes (seeding containers/wells) converge into one final node (output channel).

There are two key parameters that determine the stochastic behavior of a Markov chain: the **transition probabilities** and the **connectivity between nodes**. Applied to our problem of directional axonal outgrowth, we can interpret junctions within the PDMS structure as nodes with specific transition probabilities, and the integration of joints determines the connectivity of our Markov chain model (see Figure 6A). In this work, we further decompose the transition probabilities at a specific node into three independent core factors: **cue gradient**, **PDMS motif designs**, and **axon-axon interactions**. This split is based on prior experience with achieving directional axonal growth in PDMS structures (PDMS motif design and axon-axon interaction) plus intuition from developmental neuroscience (cue gradient).

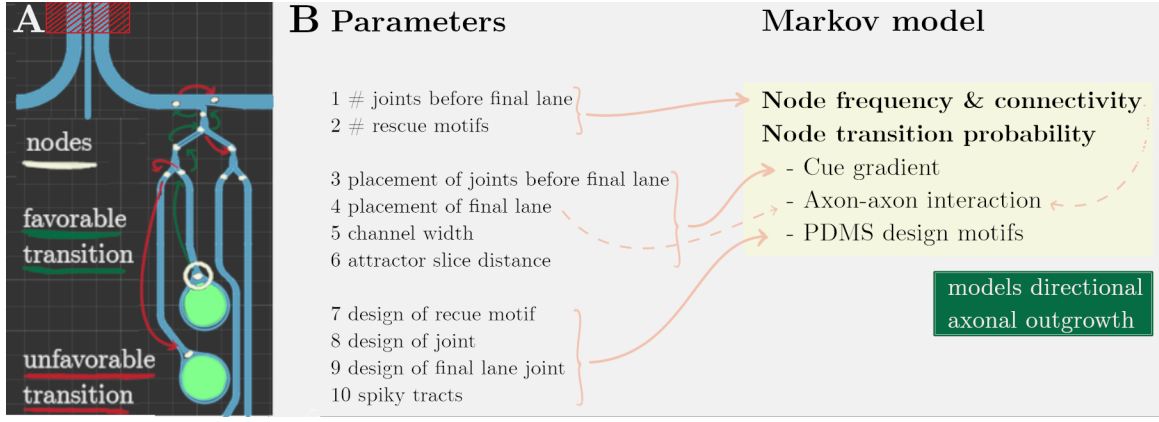


Figure 6: A: Transitions through the PDMS structure, beige indicates nodes, beige circle the starting node for this example. B: Parameter to Markov model correspondence.

4.2.1 Grouping dependent parameters based on the Markov model

The multitude of parameters and potential PDMS designs was the chief motivation behind the Markov model. Rather than utilizing the Markovian interpretation of the problem for simulation of potential PDMS designs, the idea here is to draw intuition about the interdependence of different design parameters to reduce the search space. The aforementioned decomposition of a Markov chain into node connectivity and transition probabilities can be employed to split the parameters into groups. By assuming that **node frequency & connectivity**, **cue gradient** and **PDMS design motifs** are independent drivers of directional axonal outgrowth, we alleviate the combinatorics problem.

The aforementioned ten PDMS design parameters intentionally map onto those components as depicted in Figure 6B. The **general connectivity** between nodes is defined by two parameters: the number of joints and the number of rescue loops. We could imagine a binary tree like structure that joints all axonal tracts to one final output, or a structure with no joints where all tracts converge into the output channel. The **cue gradient** present at each junction is primarily defined by the location of the junction. Early junctions will have higher concentrations of neighboring wells, later ones will exhibit higher concentrations of molecules emitted by the thalamic tissue placed above the output channel. The concentration of molecules is further affected by channel width and the distance at which the thalamic attractor is placed. Details in the PDMS designs, eg. design of rescue loops, normal joints, final lane joints and the integration of spiky tracts are summarized under **PDMS design motifs** in the Markov model. Our last component, axon-axon interaction doesn't seem to be immediately affected by any of our parameters, except indirectly the placement of the final lane. The exact relation between parameters and their Markovian interpretation is developed in the next section.

4.3 Deriving parameter value combinations from the Markov model

From the Markov model interpretation we obtain three separate factors to optimize: the **connectivity between channels (i)** until converging into the final output channel, the **cue gradient at channel junctions (ii)**, and the details in the **PDMS motif designs themselves (iv)**. Finally, we may try to come up with parameter value combinations that implicitly yield higher directional growth through **axon-axon interaction (iii)**. The following 20 designs (Figure 7; see Suppl. figures for all designs) aim to address specific questions about the value of certain factors for these four sub-components i-iv. The next section goes into the rationale.

design	# joints before final lane	# rescue motifs	placement of joints before final lane		placement of final lane		channel width	attractor slice distance	design of recue motif	design of joint	design of final lane joint	spiky tracts	notes
	1	2	3	4	5	6	7	8	9	10	cue gradient: red=steep thalamix attractor		
{ 1 2 3 4 }	0	0	NA	late	8u	short		3u			None	Exp1: Assume that final lane joints exhibit favorable transition probabilities, prior joints are only increasing cross-growth risk. Designs decrease in thalamic attractor concentration, testing how much is required.	
	0	0	NA	late	4u	short							
	0	0	NA	late	1.5u	short							
	0	0	NA	late	8u	long							
{ 5 6 7 8 }	1	0	late	late	8u	short					Exp2: Designs assume that prior joints are useful because the favorable trans. probability increases at the output lane when fewer channels arrive there. Early joints have lower thalamic attractor concentration, but more neurotrophic factors from neighbouring wells, supporting initial outgrowth.		
	3	0	late	late	8u	short							
	1	0	early	late	8u	short		-//-					
	3	0	early	late	8u	short							
{ 9 10 11 12 }	0	1	NA	late	8u	short					Exp3: First two assume 2-joints are unfavorable, second two assume they are helpful. Here, Rescue loops are integrated in this design, assuming that they have a larger positive effects, than risking reverse-growth. Cue gradient, again, decreases through four designs		
	0	3	NA	late	8u	short							
	1	1	early	late	8u	short							
	1	3	early	late	8u	short							
{ 13 14 15 16 }					5u			1.5u			None	Exp4: Test specific motifs. 13 & 14 test opening diameter (including final lane). 15 relies on joints with tangent angles. 16 omits 90 degree turns. Cue gradient is affected by opening diameter, but since both final lane- and 2-joints are adjusted, the ratio between thalamic and neighbouring attractors should be constant	
					1.5u			3u			None		
					3u			3u			None		
					3u			3u			None		
{ 17 18 19 20 }					3u			3u			Included	Exp5: Test further designs (continuation of Exp4) joints in 17 have a specific inlay, 18 reiesy on spikes on edges that are unpreferred for growth. Last two designs try a wide and slim final lane joints.	
					3u			3u			None		
					3u			3u			None		
					3u			3u			None		

Figure 7: Structure designs parameter overview. Changes in parameter values and most promising designs (left column) are highlighted in red.

4.3.1 i: Node frequency & connectivity

The connectivity between channels is an interesting parameter to consider. Generally speaking, each node where two channels are joined into one poses a risk as the axon could make the wrong transition. Even if the joint has very favorable transition probabilities towards the output channel, let's say $p_{prefTrans} = 0.9$, it still seems optimal to stack as few as possible, since the joint event of making n correct transitions decays exponentially with n : $p_{prefTrans}^n$. The PDMS structure with minimal joints is to simply have all source nodes converge into the output channel with no prior joints. However, when considering the exact potential transitions at the converging final channel, it becomes less clear which connectivity is optimal: If we have all channels converge into the output channel with no prior joints, we may increase the probability of unfavorable transitions at that final joint. In other words, $p_{unprefTrans}$ at the final joint may increase with the number of channels converging into the output channel. As the extend of this potential effect is hard to predict, we want to empirically test how many joints should be integrated prior to the final lane. In **experiment 2**, design **5 & 7** integrate a single joint, design **6 & 8** three joints (Figure 7). It should also be noted, that joining channels reduces the required space at the final lane, thus implicitly allowing for higher density.

When thinking about optimal connectivity, rescue motifs also need to be considered. The idea behind them is to redirect axons that made unfavorable transitions back on a favorable trajectory. We are again in a tradeoff situation since rescue loops also pose a risk for unfavorable transitions of correctly growing axons, slowing them down or reducing the number of axons arriving in the output channel. The optimal number of rescue structures before a joint is explored in **experiment 3** with designs **10 & 12** implementing three rescue loops, and designs **9 & 11** implementing one. To rule out dependance with the number-joints-parameters, the designs 9 and 10 don't have a joint, 11 and 12 have one build in.

Note that all designs in experiment 2 omit rescue loops, and all designs in experiment 1 additionally omit normal junctions. Therefore, we may also draw conclusions from comparing designs 1-4, designs 5-8 and designs 9-12 in their ability to achieve directional growth. This kind of comparison is intended to be done between the most promising candidate designs from each experiment, namely design 1, 6 and 12 (highlighted in Figure 7). Design 12 is particularly special because it combines all the default parameter values, meaning it implements the parameter instantiations that we expect to be the most promising from a conservative view. While the conceptional Markov model implies independent groups of parameters, we still need to instantiate each of the non-varied parameters with the most promising and safe (default) values .

As mentioned in the implementation of general design goals (section 3.1), we have two versions of each design, one less dense design fitting the glassMEA, and one more dense design intended for high-throughput optical screening. The two versions are equal in terms of the parameter values they implement, however they do differ with respect to channel density. For the analysis of node frequency and connectivity in these two versions, we need to keep in mind that the higher density design exhibits more joints and therefore a higher chance of making un-preferred transitions.

4.3.2 ii: Transition probabilities - cue gradient

The connectivity between nodes forms the basis of the transition process, however the transition probabilities at each node are the more low-level drivers of directional axonal outgrowth. In real biological systems, the concentration gradients of attracting-, and repulsive molecules are the primary factors determining directional axonal growth. Thus, at each junction, we need to consider the concentration gradient of attractors axons are exposed to at that particular node. In **experiment 1**, the general significance of the cue gradient is tested by comparing design **1 & 4** which differ in the attractor slice distance parameter. We also expect that the axon tract width significantly affects the cue gradient at a particular junction. The designs **2 & 3** use tract widths of 4 um and 1.5 um, instead of the default 8 um. This is likely going to affect the speed of axonal outgrowth metric as well.

As stated in the introduction, we place thalamic tissue on top of the output channel to have potential secreted attractors diffuse into the output channel. From the output channel, potential attractor cues diffuse towards the seeding wells. Besides this concentration gradient, the cells located in the seeding wells may emit neurotrophic factors. From a simple, qualitative view, the cue gradient at a junction is determined by the distance towards the thalamic attractor and the distance to other seeding wells. It follows intuitively that we prefer junctions that are closest to the thalamic attractor, and most distant to other seeding wells. Such a junction would exhibit favorable transition probabilities towards the output channel. This line of

reasoning would imply late joints to be the optimal solution. However, there might be an advantage to early joints as well. The thalamic attractor concentration reaching the seeding well might be insufficient to trigger axonal outgrowth. Early joining of two channels may be necessary to initialize axonal growth in a seeding well. In this scenario, the higher concentrated neurotrophic factors of a connected (or potentially multiple) neighboring well could act as an initial growth trigger. Of course, once this axon reaches the junction, the cue gradient of the thalamic attractor should be more dominant than the initial growth trigger from the neighboring well such that the right transition is made. This argument was the reason to default to an early placement of the normal joint, ensuring that there will be initial growth. In summary, any early junction may support initial growth but pose a risk for cross growth, while late junctions have more favorable cue gradients that positively affect transition probabilities. Since the optimal balance between these two opposing factors is unknown, the placement-of-joints parameter is varied throughout **experiment 2 and 3**. In Figure 7, this is visualized by the red bar in the notes section.

The placement of the final lane is a somewhat deviant parameter because all the new PDMS designs share the same value, namely a late placement of the final lane. In contrast, the current design has the final lane placed early (see Figure 5). This placement affects the cue gradient just as much as varying the normal two-channel joint placement, however, an early placement of the final lane comes with several disadvantages, which is why it's been kept 'late'. First, the absolute amount of thalamic attractors reaching the seeding wells is lower when the lane is placed early because the final lane junctions are further away from the output channel. Hence, the thalamic cue gradient is worse. Second, it is more time consuming to vary in CAD because spacing becomes more constraint, and third there might be negative effects on axon-axon interaction (see next section for details). This is why we rely on the two channel joint placement as the primary turning knob for changing the cue gradient.

As a last general point, for the future analysis of the structures, one should always keep in mind that the cue gradient naturally varies across equivalent junctions in the structure. The more a seeding well lays at the outside of the array (further away from the output channel), the lower the thalamic attractor concentration. Thus, each PDMS structure has an inherent variance in the cue gradient across seeding wells. If the cue gradient is a strong driver of directional growth, we expect that cross talk frequency within a structure will be lowest at the center (close to output channel).

4.3.3 iii: Transition probabilities - axon-axon interaction

A far less controllable yet crucial factor determining axon growth behavior through the structure is the presence of other axons. If an axon hits another one it will likely attach and grow along the preexisting axon. We may therefore think of preexisting axons as dynamic edges that appear over time. How can we make use of this behavior to increase directional growth? The designed structures indirectly make use of this through the late placement of the final lane. The detailed explanation behind this is rather cumbersome, and therefore excluded. In short, a late final lane has a lower probability that dynamically growing axons form new, unfavorable edges that most likely decrease directional growth. Placing the final lane late in some way reduces the impact of axon-axon interaction.

It could also be that more joints before the final lane, eg. design 10 and 12, are useful because they decrease the number of inputs to the final lane reducing the effects of possibly messy axon-axon interaction. All in all, axon-axon interaction remains a randomizing factor that is difficult to predict.

4.3.4 iv: Transition probabilities - PDMS design motifs

Together with the cue gradient, this work assumes the details in the PDMS tract/joint design to be the major driver of directing axonal growth. In fact, the tract and joint design may very well be more important than the cue gradient. Forro *et al.* 2018 stomach designs are solely relying on guiding structures to achieve highly unidirectional growth. This article and theoretically proposed structures from our lab were used as a foundation to develop new design motifs.

At the lowest level, we assume that axons prefer adhesion to an edge. As long as this edge is continuous and no sharp turns are encountered, the axon will follow the edge. Another empirically confirmed behavior of axonal growth is that the angle at which a freely growing axons hits an obstacle determines in which direction it will continue to grow. If an axon hits an edge with 135°, it will change its growth direction to 45°, following the encountered edge. Our PDMS motifs were designed based on those two observations.

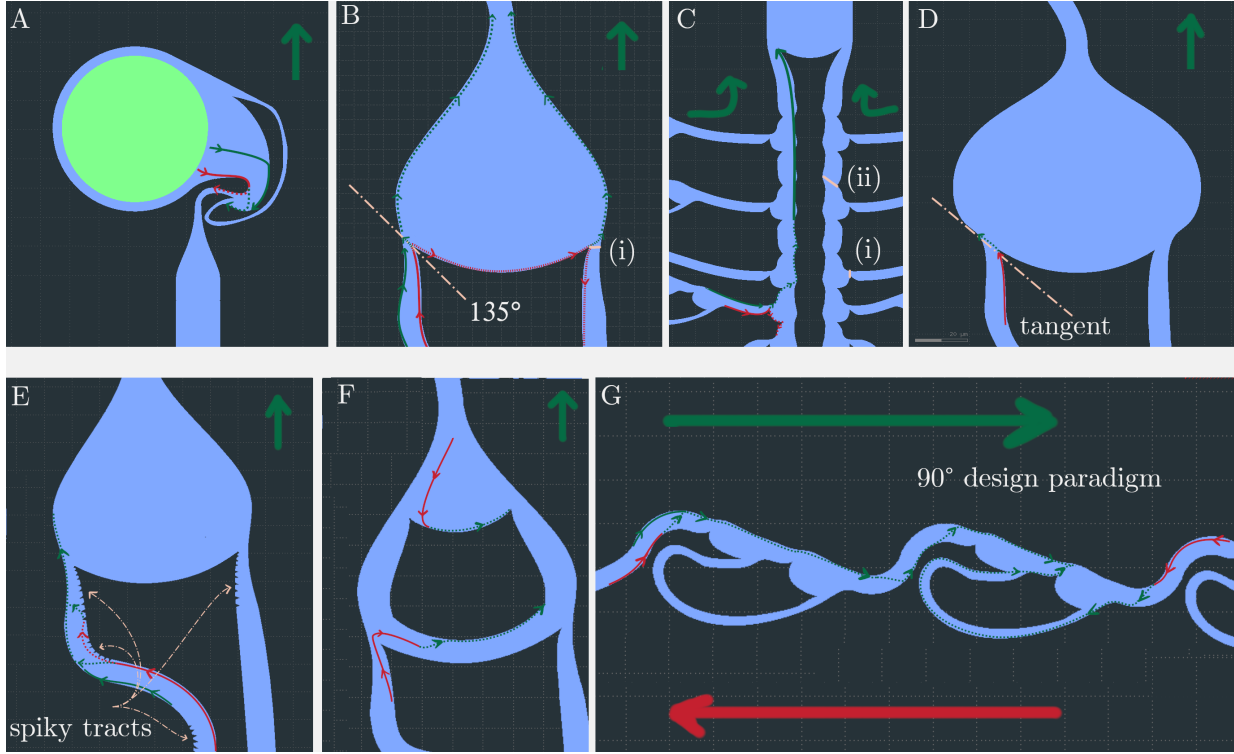


Figure 8: Implemented design motifs. Again, blue refers to channels 6 um high, light green represents an opening. The large red and green arrows outside the structures indicate the generally desired directionality. Dark green arrows in the structures mark favorable growth in preferred direction, red arrows the opposite. A: Stomach structure from Forro *et al.* 2018. B: Normal 2-joint, (i) indicates the opening diameter in the design. C: Final lane design, (ii) is the diameter from the outer the inner edge. D: 2-joint with tangent continuation of the tract. E: Spiky tracts in 2-joint. Note that the placement of these spikes is not limited to the 2-joint. G: Rescue loops with 90° turns attached.

At the center of our designs lies the idea of preferred and un-preferred edges in the growth tract. We always try to make axons grow on the preferred edge because, here, the probability of making correct transitions is higher (Figure 8, green tracts). We are often in a situation where we need to send axons from the un-preferred edge to the opposing, preferred one. This is achieved by implementing 'un-preferred' motifs at the current edge that will likely lead to detachment of the axon, making it transition to the opposing edge. For example, the stomach structures described in Forro *et al.* 2018 rely on a sharp radius of the un-preferred edge (Figure 8A), leading to a transition towards the preferred one such that axons don't grow towards the bottom into the input channel. The joints in our designs work in a similar way: an arc-shaped edge followed by a sharp discontinuation of the tract induces a transition to the opposing, preferred edge (Figure 8B). While a small opening in this joint design may act like a valve and exhibit higher likelihood to switch edges, the size constraint may significantly slow down axonal growth. On the other hand, larger openings may be less favorable for transitioning edges, however, general outgrowth speed should increase. The default distance the axon needs to cover when transitioning to the other edge is 3 um. In design **13 & 14**, openings of 1.5 um and 5 um are tested (Figure 8B (i)). The same situation applies to the final lane. Here, we require a wider tract as multiple axons need to fit in. To find the optimal parameter value here, the final tract width is made smaller in design **19**, and wider in design **20** (Figure 8C (ii)).

In the default joint, the axon hits the preferred edge with an angle of 135°, promoting growth in the preferred direction. In contrast, design **15** makes the axons hit the opposing edge tangentially, which may yield better transition probabilities and therefore higher directional growth (Figure 8D).

Another parameter in our designs is the inclusion of spiky tracts at the un-preferred edge (Figure 8E). Following the design paradigm above, we try to drive the axons towards the preferred edge. In design **17**,

the critical regions of the un-preferred edge are covered with spikes such that the likelihood of growing on that un-preferred edge is decreased.

Both the 2-joint and final lane joint implement a concave inner edge to drive axons that hit this edge towards the preferred direction again. In design **18**, this idea of a rescue structure within a joint is taken a step further by inserting a motif with favorable transition edges (Figure 8F). Again, we may achieve better transition probabilities by using this joint modification.

The last impactful motif was the design of the rescue loops. These motifs are intended to redirect wrongly growing axons that made un-preferred transitions back towards a preferred trajectory (Figure 8G). One such rescue loop should have the property to redirect axons from one direction, while not affecting axons growing in the opposite, correct direction. This is achieved with the angles by which the loop is entered. Also, the loops are always proceeded and followed up by a 90° turn. These adjacent motifs are motivated by the observation that axons avoid edges with a tight radius and will instead transition to the edge with the larger radius. We make use of this behavior to drive axons towards the preferred edge as illustrated in Figure 8G. The 90° turn achieves that axons that grow in the correct direction will not grow on the edge with the rescue loops, while those growing in the opposing direction are driven into the rescue loop. This principle is used beyond just rescue loops. Both the normal joint and final lane joint are proceeded by a 90° turns such that axons enter the joint on the preferred edge.

While these motifs should improve directionality in the structures, the multitude of 90° turns may also result in diminished axonal growth speed. Therefore, we include design **16** which omits all 90° turns. The eight structures 13-20 targeting motif designs are compared in **experiment 4 and 5**.

4.4 Further experiments

The 20 designs described above have the primary aim to promote directional growth towards the output channel. At the same time, as pointed out in the general design goals (section 3), the wafer design should also address secondary objectives. For example, including specific layouts of structures that enable a particular experiment. In the figure below, the planned experimental setups are illustrated.

Experiments 1-5 were mentioned in the section above. These 8-stack layouts are specifically targeted towards finding structures that minimize channel cross talk (Figure 9 (i)). Each of these 20 designs has a port that fits the glassMEA in a 2-stack configuration (Figure 9 (ii)). For the following experiments, the same set of the five most promising designs are used, namely design 1, 6, 12, 14, and 16. These cover a wide range of parameter values such that at least a subset of them should perform well in experiments that go beyond the optimization of cross talk. The first of these is **experiment 6**. Here, the optimal cell container is tested, a parameter that likely affects neural viability and axonal output growth speed & frequency (Figure 9 (iii)). Besides the default of using explant containers with dimensions 500 um x 300 um, smaller wells with diameters of 90 and 180 um are tested. These are seeded using a single cell suspension of retinal ganglion cells (RGC).

In **experiment 7**, we connect the output channels of two opposing structures to test the attractive properties between them (Figure 9 (iv)). This experiment was motivated by the observation that two contralaterally growing axon bundles form a nerve-like structure, potentially increasing functional efficacy and stability. Once this structure has formed in the output channel, we plan to cut off one design to observe whether the opposing structure maintains the functional nerve-like structure. If this is indeed the case, this method would become the default for building our biohybrid interface.

Lastly, we introduce a structure layout that would allow us to demonstrate *in vitro* innervation of thalamic tissue, **experiment 8** (Figure 9 (v)). Again, we use the 5-stack of the most promising designs as the base. What is special for this setup, is that we attach a stomach structure at the end of the 3 mm output channel. We would place a piece of thalamic tissue (ideally only LGN) into the stomach structure such that thalamic axons do not grow out but RGC axons can enter the structure and synapse onto the tissue piece. Because this experiment is so central, we made a port that fits the glassMEA as well. Here, we could also test how rhythmic oscillatory stimulation affects RGC growth behavior, as this is observed in natural formation of the optic pathway.

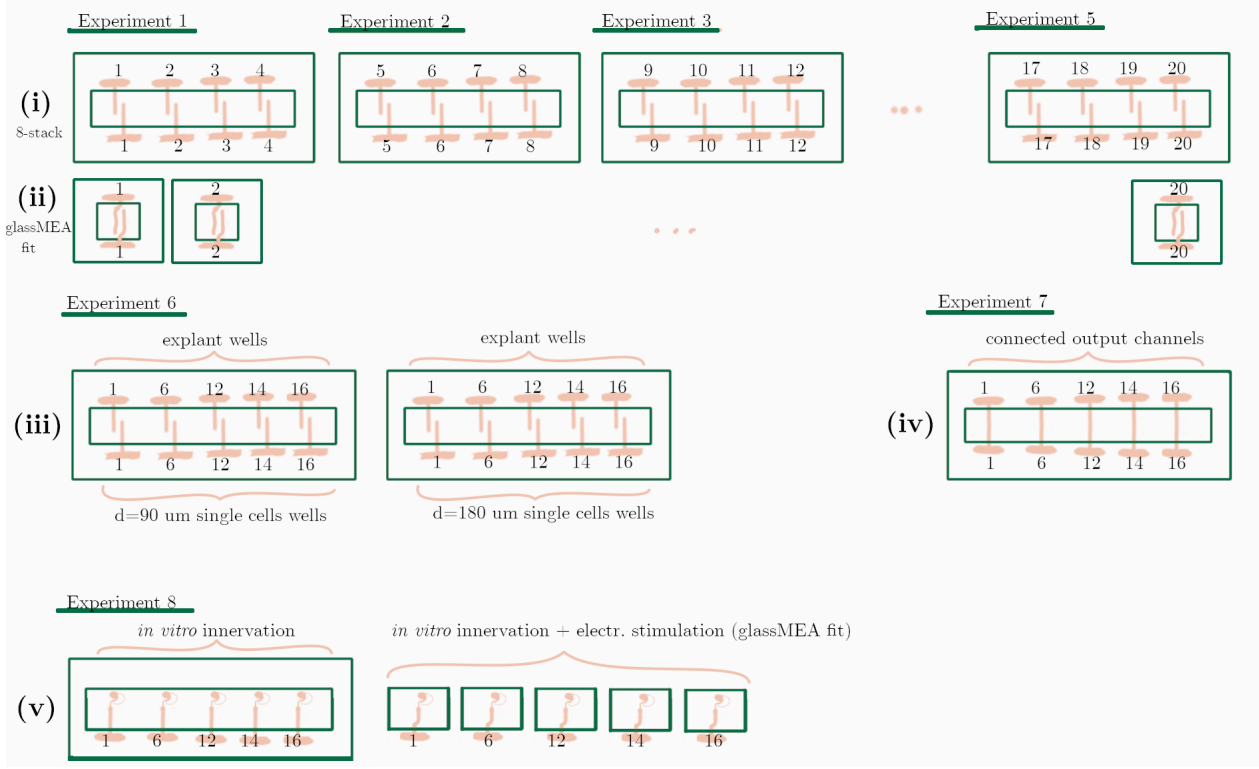


Figure 9: Outline of experimental setups. Green borders indicate PDMS frames that compartmentalize the well. These are glued to the implant.

5 Discussion

In this short project, we formulated an engineering process framework to handle the complexity in building the bioMEA. Taking this framework into practice, we designed a new PDMS wafer to increase experimental throughput and implement experiment-specific layouts. The wafer is composed of 20 new PDMS structures that optimize directional growth through the channel system. For each of these designs, a ported version that fits the glassMEA is placed on the wafer as well. Especially the engineering framework is a significant contribution to succeeding with the endeavour of building a stimulating brain machine interface in the long run. Using the new 8-stack and 2-stack PDMS structures, we can now systematically test parameters, starting with finding the structures that exhibit minimal channel cross talk. Once we receive the fabricated PDMS structures, the crucially important next step is to develop reliable, reproducible, and efficient screening methods that quantify the metrics, starting with channel cross talk.

6 Supplementary Information

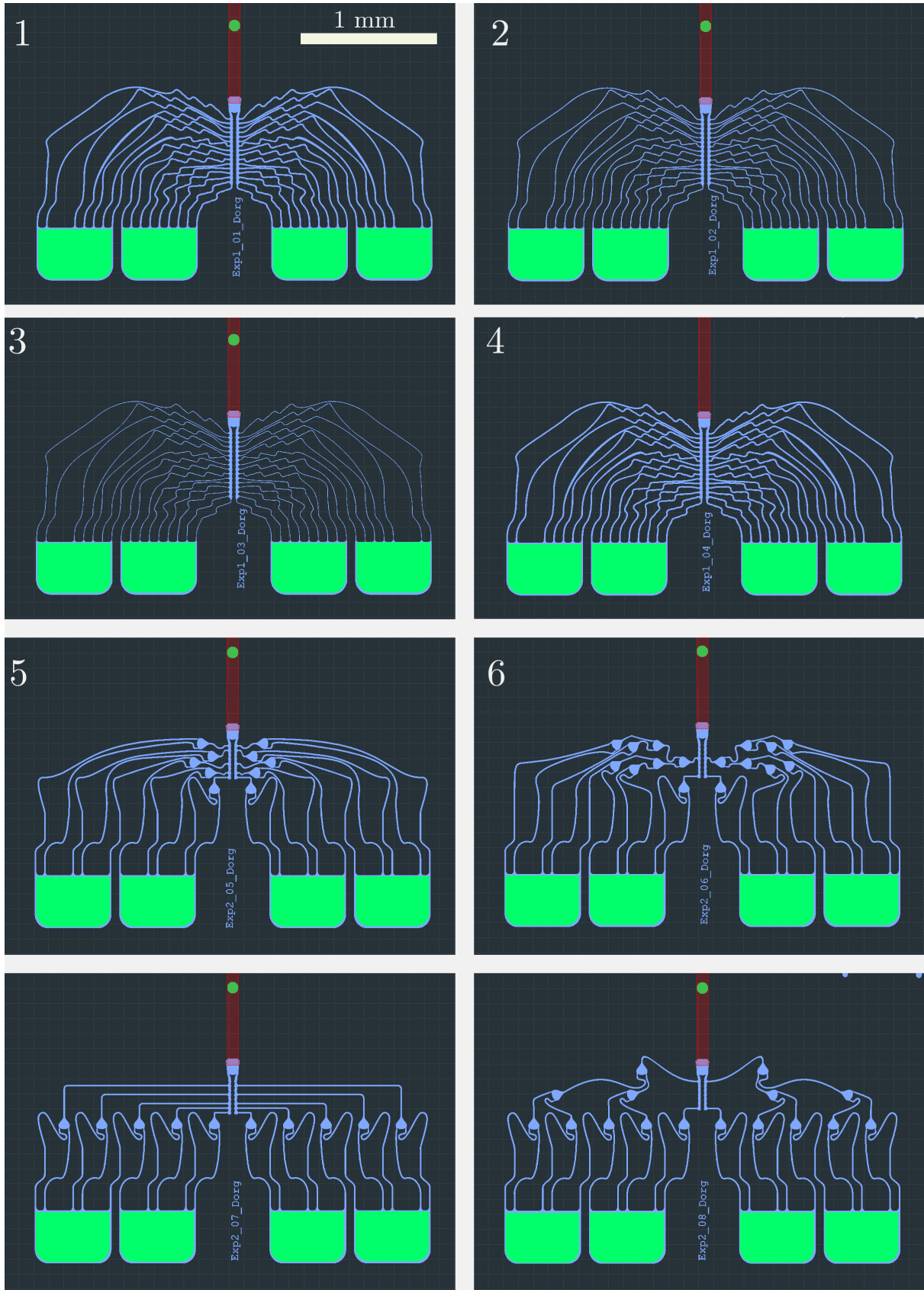


Figure 10: Designs 1-8

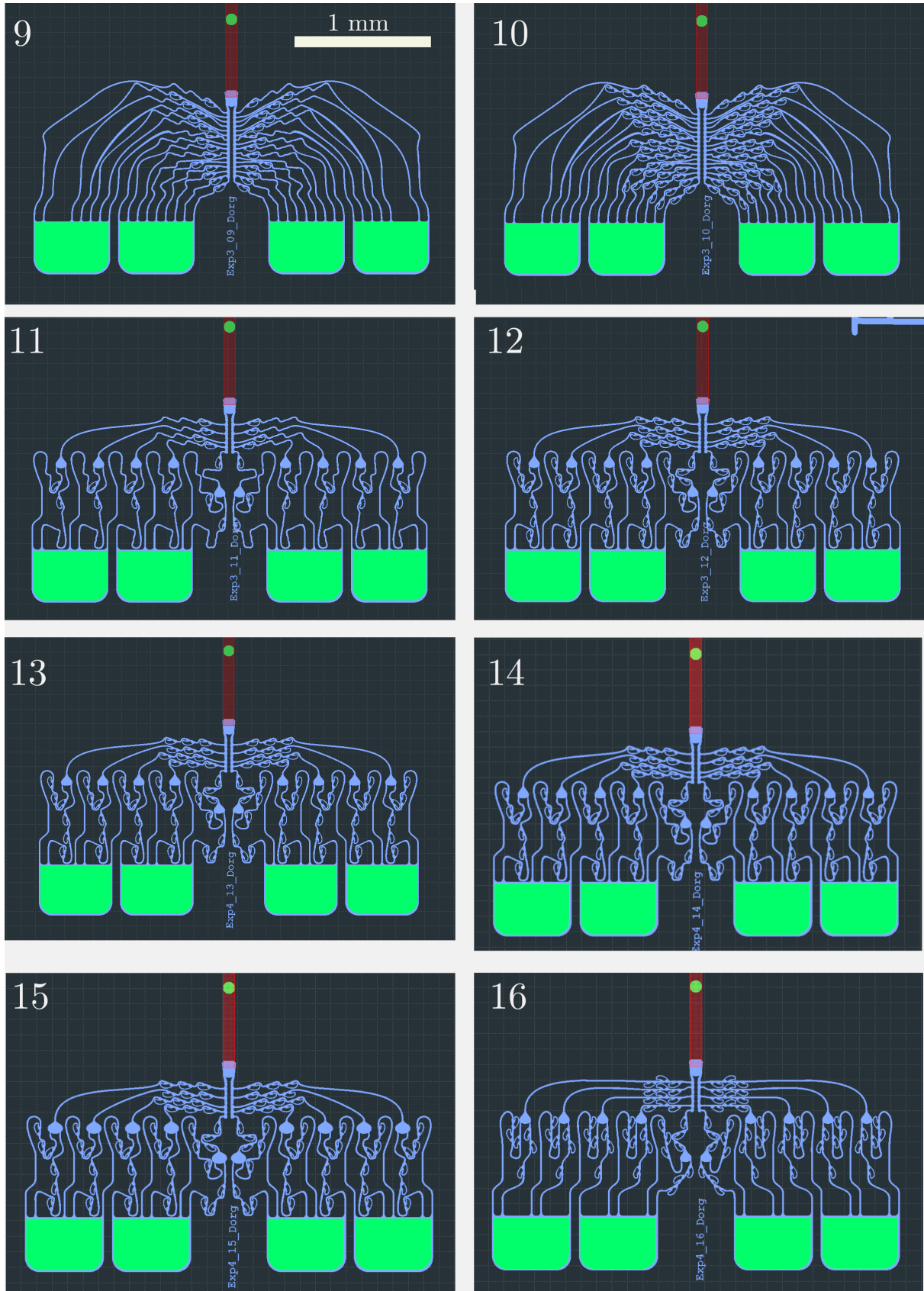


Figure 11: Designs 9-16

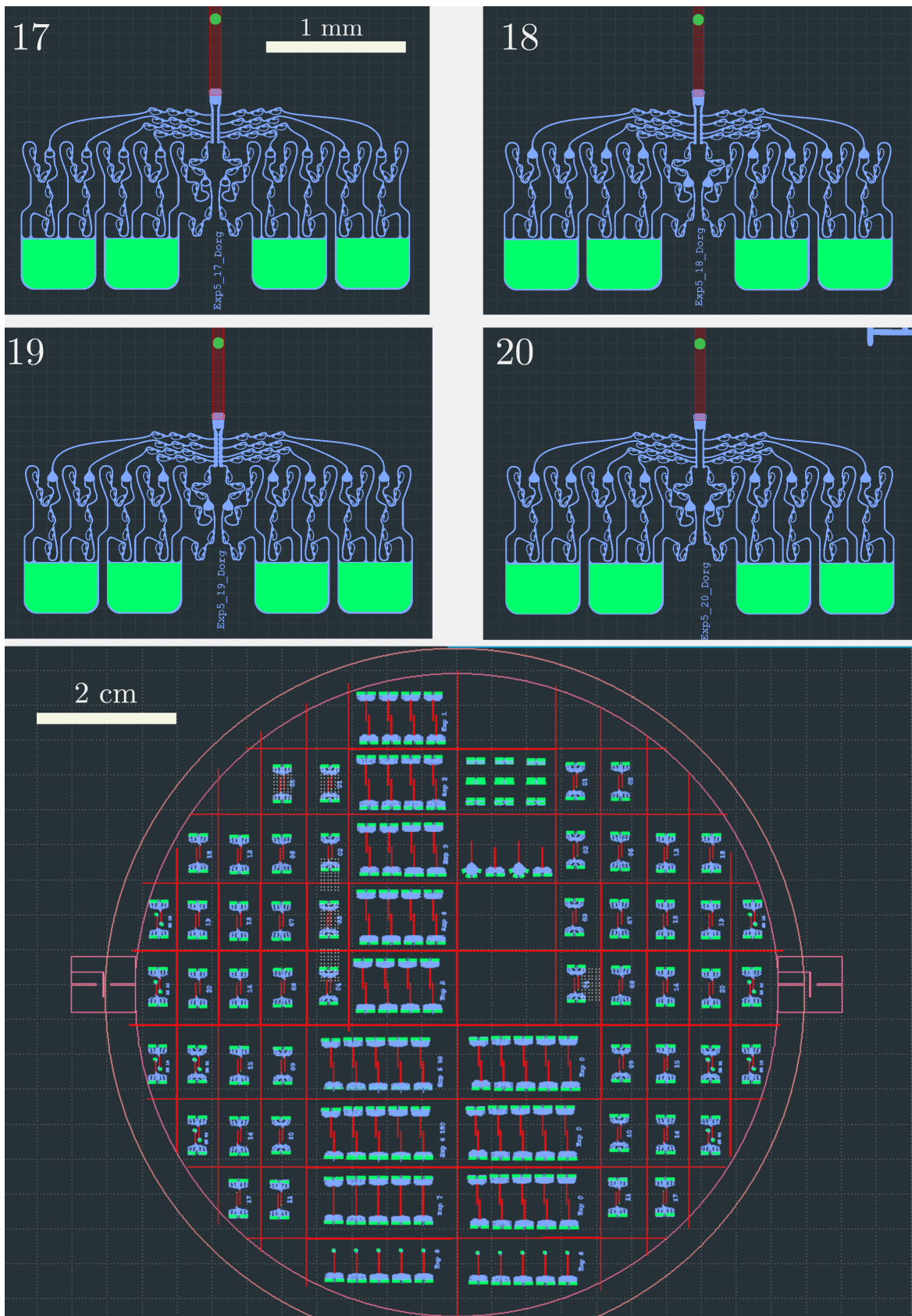


Figure 12: Designs 17-20. Screenshot of entire wafer.

21

250 um

